

Synthesis and characterization of cobalt-iron (bimetallic) nanocatalyst via strong electrostatic adsorption (SEA) method

By

KHAIRULAMIN BIN AHMAD

Dissertation submitted in partial fulfillment of

the requirement for the

Bachelor of Engineering (Hons)

(Chemical Engineering)

JANUARY 2012

Universiti Teknologi PETRONAS

Bandar Seri Iskandar

31750 Tronoh

Perak Darul Ridzuan

CERTIFICATION OF APPROVAL

Synthesis and characterization of cobalt-iron (bimetallic) nanocatalyst via strong electrostatic adsorption (SEA) method

By:

KHAIRULAMIN BIN AHMAD

**A project dissertation submitted to the
Chemical Engineering Programme
Universiti Teknologi PETRONAS
in partially fulfillment of the requirement for the
BACHELOR OF ENGINEERING (Hons)
(CHEMICAL ENGINEERING)**

Approved by,



(AP DR. NOOR ASMAWATI BT M ZABIDI)

**Assoc. Prof. Dr. Noor Asmawati Mohd. Z.
Head
Centralized Analytical Laboratory
Universiti Teknologi PETRONAS**

UNIVERSITI TEKNOLOGI PETRONAS

TRONOH, PERAK

JANUARY 2012

CERTIFICATION OF ORIGINALITY

This is to certify that I am responsible for the work submitted in this project, that the original work is my own except as specified in the references and the acknowledgements, and that the original work contained herein have not been undertaken or done by unspecified sources or persons.



KHAIRULAMIN BIN AHMAD

ACKNOWLEDEMENT

First and foremost, highest thanks to The Almighty, the source of life, wisdom and hope for giving the author the strength and patience to pursue and complete this Final Year Project within the time frame.

The author's utmost gratitude goes to the author's supervisor, Associate Professor Dr. Noor Asmawati Bt M Zabidi for the informative supervision and valuable knowledge throughout the project. Without her guidance and patience, the author would not be succeeded to complete the project. Thank you to the Final Year Research Project Coordinator, Dr. Lukman Bin Ismail for providing all important information throughout this project.

The author's sincere thanks to Chemical Engineering Department of Universiti Teknologi PETRONAS (UTP) for providing this chance to undertake this remarkable final year project. Special thanks also to all contributors for the kind cooperation and assistance in tutoring the author in conducting this project.

Last but not least, special credit goes to the author's parents, family members and friends, who had dedicatedly provided the author with additional support and encouragement throughout this project either directly or indirectly. Thanks again to all, your kindness and helps will always be remembered.

*The project is funded by Fundamental Research Grant Scheme, Ministry of Higher Education Malaysia (FRGS No: FRGS/2/2010/SG/UTP/02/3).

Table of Contents

Table of Contents	i
List of Figures	iii
List of Tables.....	iv
ABSTRACT	1
CHAPTER 1	2
1.1 Background Study	2
1.2 Problem Statement	3
1.3 Objectives	3
1.4 Scope of Work.....	4
1.5 Relevancy of the Project.....	4
1.6 Feasibility of the Project.....	4
CHAPTER 2	5
2.1 Introduction to Fischer-Tropsch synthesis (FTS).....	5
Reaction mechanisms:	6
Process conditions:	6
2.2 Catalysts for Fischer-Tropsch Synthesis	7
2.3 Strong electrostatic adsorption (SEA).....	10
CHAPTER 3	12
3.1 Methodology	12
3.2 Experimental	12
3.2.1 Treatment of CNTs	12
3.2.2 Catalyst preparation	14
3.2.3 Catalysts characterization	15

3.3 Tools Required	16
3.3.1 Chemicals.....	16
3.3.2 Equipment.....	16
3.4 Project’s Gantt chart and key milestone.....	16
CHAPTER 4	17
4.1 Transmission Electron Microscope (TEM)	17
4.2 Field Emission Scanning Electron Microscope (FESEM-EDX)	22
4.3 Surface area analyzer (BET)	25
4.4 Temperature programmed reduction (TPR).....	26
4.5 Micro-tubular fixed-bed reactor	27
CHAPTER 5	30
5.1 Conclusion.....	30
5.2 Recommendation.....	30
REFERENCES.....	31

List of Figures

<i>Figure 1: Mechanism of Fischer-Tropsch Synthesis</i>	5
<i>Figure 2: Mechanism of strong electrostatic adsorption (SEA) method</i>	11
<i>Figure 3: Flow chart of experiment procedure</i>	12
<i>Figure 4: CNTs pretreatment process</i>	13
<i>Figure 5: Washing process</i>	13
<i>Figure 6: Stirred the solution for an hour</i>	14
<i>Figure 7: Calcination process using furnace Carbolite</i>	15
<i>Figure 8: TEM image of the 100Co/CNT catalyst</i>	17
<i>Figure 9: TEM image of the 90Co10Fe/CNT catalyst</i>	17
<i>Figure 10: TEM image of the 80Co20Fe/CNT catalyst</i>	17
<i>Figure 11: TEM image of the 70Co30Fe/CNT catalyst</i>	17
<i>Figure 12: Particles size distribution for 100Co/CNT catalyst (inside CNT)</i>	18
<i>Figure 13: Particles size distribution for 90Co10Fe/CNT catalyst (inside CNT)</i>	19
<i>Figure 14: Particles size distribution for 90Co10Fe/CNT catalyst (outside CNT)</i>	19
<i>Figure 15: Particles size distribution for 80Co20Fe/CNT catalyst (inside CNT)</i>	20
<i>Figure 16: Particles size distribution for 80Co20Fe/CNT catalyst (outside CNT)</i>	20
<i>Figure 17: Particles size distribution for 70Co30Fe/CNT catalyst (inside CNT)</i>	21
<i>Figure 18: Particles size distribution for 70Co30Fe/CNT catalyst (outside CNT)</i>	21
<i>Figure 19 : SEM image of the 100Co/CNT catalyst</i>	22
<i>Figure 20 : SEM image of the 90Co10Fe/CNT catalyst</i>	22
<i>Figure 21 : SEM image of the 80Co20Fe/CNT catalyst</i>	22
<i>Figure 22: SEM image of the 70Co30Fe/CNT catalyst</i>	22
<i>Figure 23 : EDX spectra of the 100Co/CNT catalyst</i>	23
<i>Figure 24: EDX spectra of the 90Co10Fe/CNT catalyst</i>	23
<i>Figure 25 : EDX spectra of the 80Co20Fe/CNT catalyst</i>	23
<i>Figure 26 : EDX spectra of the 70Co30Fe/CNT catalyst</i>	23
<i>Figure 27: TPR profiles of 100Co/CNT, 90Co10Fe/CNT, 80Co20Fe/CNT and 70Co30Fe/CNT</i>	26
<i>Figure 28: Gas chromatogram showing analysis of H₂, CO and hydrocarbon products</i>	28
<i>Figure 29: %CO conversion for catalysts</i>	29

Figure 30 : Product selectivity of catalysts.....29

List of Tables

Table 1: Comparison of Cobalt and Iron FT Catalysts8

Table 2: Composition of Fe VS Co (5 wt. %).....14

Table 3: Numbers of particles for each sample18

Table 4: percentage of element for each composition24

Table 5 : BET surface area and porosity data for catalysts.25

Table 6: %CO conversion and product selectivity of catalysts28

ABSTRACT

This project focuses on preparation of Fischer-Tropsch (FT) catalyst by using strong electrostatic adsorption (SEA) method. The simple catalyst synthesis method of strong electrostatic adsorption is applied to cobalt-iron (bimetallic) system on carbon nanotubes support. The pH value plays an important role in the deposition of metal precursor using SEA method. Iron was incorporated into cobalt at ratio of 10, 20 and 30 wt%. The physico-chemical properties, FT activity and selectivity of the bimetallic catalysts were analyzed and compared with those of monometallic cobalt catalysts at similar operating conditions ($H_2/CO = 2:1$ molar ratio, $P = \text{Atmospheric}$ and $T = 220$ °C). The average size of metal oxide particles deposited on the inner and outer walls of the CNTs was $6 \pm 1.5 \text{ nm}$ and $6.5 \pm 3 \text{ nm}$, respectively. Using the $90\text{Co}10\text{Fe}/\text{CNT}$ catalyst, the CO conversion was 2.5% and C_5^+ selectivity was 0.85%. Other composition did not produce C_5^+ hydrocarbon.

CHAPTER 1

INTRODUCTION

1.1 Background Study

In the paper by Andrei Y. Khodakov, Wei Chu, and Pascal Fongarland, it stated that the first experiment on catalytic hydrogenation of carbon monoxide was carried out at the beginning of 20th century. In 1902, Sabatier and Senderens synthesized methane from a mixture of CO or CO₂ with hydrogen. The reaction was performed on cobalt or nickel catalysts at temperatures of 473-453 K and under atmospheric pressure. In 1922, Hans Fischer and Franz Tropsch proposed the Synthol process, which gave, under high pressure (>100 bar), a mixture of aliphatic oxygenated compounds via reaction of carbon monoxide with hydrogen over alkalized iron chips at 673 K. This product was transformed after heating under pressure into "Synthine", a mixture of hydrocarbons. Important progress in the development of Fischer-Tropsch (FT) synthesis was made in 1923. It was found that *more and more heavy hydrocarbons could be produced when the Synthol process was conducted at lower pressure (7 bar)*. Heavy hydrocarbons were the main products of carbon monoxide hydrogenation. [Andrei Y. Khodakov, 2007]

In 1993, Shell Bintulu (12 500 barrels per day) (bpd) plant came into operation. In June 2006, the Sasol Oryx 34 000 bpd plant was inaugurated. SasolChevron is currently building its Escarvos GTL plant in Nigeria. Shell and Exxon signed the agreement on building 140 000 and 150 000 bpd GTL-FT plants in Qatar. Thus, after several decades of research and development, FT technology has finally come to the stage of full-scale industry and worldwide commercialization.

Nowadays, Fischer-Tropsch synthesis has been developing in oil and gas industry. The global resurgence of interest in FT synthesis has been primarily driven by the problems of utilization of stranded gas, diversification of sources of fossil fuels, and environmental concerns. The abundant reserves of natural gas in many parts of the world have made it attractive to commission new plants based on FT technology.

Synthetic liquid fuels generally have a very low content of sulfur and aromatic compounds compared to gasoline or diesel from crude oil. FT synthesis has been considered as a part of gas to liquids (GTL) technology, which converts natural and associated gases to more valuable middle distillates and lubricants. This method is one of the alternative ways to produce hydrocarbons and also can be considered as one of the green technology [Andrei Y. Khodakov, 2007].

There are few methods to synthesize the nanocatalysts for the FT synthesis. The methods are impregnations, precipitation, sol-gel, plasma, colloidal, micro emulsion, strong electrostatic adsorption (SEA) [Andrei Y. Khodakov, 2007]. The different method will have different catalyst performance. There are several important steps in the preparation of the catalyst which are choice of appropriate catalyst support, choice of method of deposition of the active phase, catalyst promotion, and oxidative and reductive treatments. The catalytic performance of FT catalysts is usually affected by different oxidizing and reducing pretreatments. The catalytic support could also influence the performance of FT catalyst. This study will focus on strong electrostatic adsorption (SEA) method.

1.2 Problem Statement

The strong electrostatic adsorption (SEA) method was used to synthesize monometallic cobalt [Chee Kai Ling, 2011]. Supported cobalt has been found to be a good choice of catalysts for FT synthesis due to potentially high activity and selectivity. However SEA method has not been used to synthesize bimetallic iron and cobalt nanocatalyst.

1.3 Objectives

The objectives of this project are to:

- To synthesize iron-cobalt (bimetallic) nanocatalyst via strong electrostatic adsorption (SEA) method on carbon nanotube (CNT).
- To characterize physical and chemical properties of cobalt-iron on CNT support.
- To do the Fischer Tropsch reaction study using cobalt-iron nanocatalyst.

1.4 Scope of Work

The scope of work includes the following:

- Conduct the experiment that is going to be used in this study.
- Synthesize 10 wt% of cobalt-iron (bimetallic) nanocatalyst on carbon nanotube.
- Synthesis 4 sample nanocatalysts that have different percentage of Co:Fe which were 100Co, 90:10, 80:20 and 70:30.
- Characterizations of the cobalt-iron bimetallic nanocatalyst using Transmission Electron Microscope (TEM), Field Emission Scanning Electron Microscope (FESEM-EDX), Surface area analyzer (BET) and Temperature-programmed reduction (TPR).
- Use micro-tubular fixed-bed reactor to study the activity and product selectivity of nanocatalysts.

1.5 Relevancy of the Project

This project is relevant because it may give a positive result on the performance of FT catalyst throughout the experimental practices by applying different catalyst synthesis method. The strong electrostatic adsorption (SEA) method is simple, logical explanation of mechanism for cobalt precursor deposition on the oxide support and should yield higher dispersion at narrow particle size distribution compared to the other methods [Jiao, 2008]. To optimize the performance of catalyst, a single metal of cobalt is combined with iron to form bimetallic system. The performance of bimetallic system will be compared with that of monometallic system.

1.6 Feasibility of the Project

The strong electrostatic adsorption (SEA) method is suitable to be done in laboratory as there are tools, equipment and also chemicals which are the main elements to determine whether this project may excel or not. The time given to conduct the experiment is also sufficient which consist of the period of preparing the catalyst and the reaction study of catalyst.

CHAPTER 2

LITERATURE REVIEW

2.1 Introduction to Fischer-Tropsch synthesis (FTS)

FTS is a set of chemical reaction that converts a mixture of carbon monoxide and hydrogen into liquid hydrocarbons. The process, a key component of gas to liquid technology, produces a petroleum substitute, typically from coal, natural gas, or biomass for use as synthetic lubrication oil and as synthetic fuel. The FTS has received intermittent attention as a source of low-sulfur diesel fuel and to address the supply or cost of petroleum-derived hydrocarbons.

In FTS, syngas CO and H₂ are converted to hydrocarbons mainly over Co or Fe based catalysts according to reaction [Andrei Y. Khodakov, 2007]:

FTS reaction

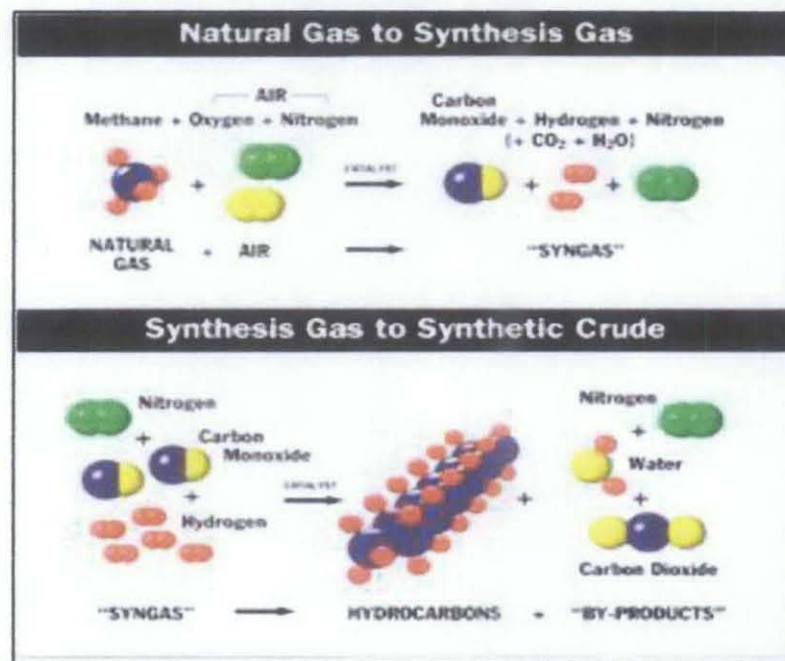
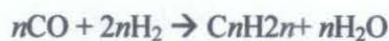


Figure 1: Mechanism of Fischer-Tropsch Synthesis

Reaction mechanisms:

The conversion of CO to alkanes involves net hydrogenation of CO, the hydrogenation of C-O bonds, and the formation of C-C bonds. Such reactions are assumed to proceed via initial formation of surface-bound metal carbonyls. The CO ligand is speculated to undergo dissociation, possibly into oxide and carbide ligands [Jiao, 2008]. Other potential intermediates are various C-1 fragments including formyl (CHO), hydroxycarbene (HCOH), hydroxymethyl (CH₂OH), methyl (CH₃), methylene (CH₂), methyldiyne (CH), and hydroxymethyldiyne (COH). Furthermore, and critical to the production of liquid fuels, are reactions that form C-C bonds, such as migratory insertion. Many related stoichiometric reactions have been simulated on discrete metal clusters, but homogeneous F-T catalysts are poorly developed and of no commercial importance [Andrei Y. Khodakov, 2007].

Process conditions:

Generally, the Fischer–Tropsch process is operated in the temperature range of 150–300 °C (302–572 °F). Higher temperatures lead to faster reactions and higher conversion rates but also tend to favor methane production. As a result, the temperature is usually maintained at the low to middle part of the range. Increasing the pressure leads to higher conversion rates and also favors formation of long-chained alkanes both of which are desirable. Typical pressures range from one to several tens of atmospheres. Even higher pressures would be favorable, but the benefits may not justify the additional costs of high-pressure equipment and higher pressures can lead to catalyst deactivation via coke formation. A variety of synthesis gas compositions can be used. For cobalt-based catalysts the optimal H₂: CO ratio is around 1.8-2.1. Iron-based catalysts promote the water-gas-shift reaction and thus can tolerate significantly lower ratios. This reactivity can be important for synthesis gas derived from coal or biomass, which tend to have relatively low H₂: CO ratios (<1) [Andrei Y. Khodakov, 2007].

Fundamental studies showed that activity of catalyst depend on the number of active sites which is number of precursor metallic particle on the support, namely number of metallic particle on the support [Den Breejen, J.P, 2009]. FTS activity is a

function of the number of metallic particle on the support surface, which is exposed to the syngas reaction [S.Sun, 2000] .This factor, depends on metallic loading, dispersion of metallic species and its reducibility.

2.2 Catalysts for Fischer-Tropsch Synthesis

All group VIII metals have noticeable activity in the hydrogenation of carbon monoxide to hydrocarbons Ruthenium followed by iron, nickel, and cobalt are the most active metals for the hydrogenation of carbon monoxide. Vannice et al. showed that the molecular average weight of hydrocarbons produced by FT synthesis decreased in the following sequence:



Thus, only ruthenium, iron, cobalt, and nickel have catalytic characteristics which allow considering them for commercial production. Nickel catalysts under practical conditions produce too much methane. Ruthenium is too expensive; moreover, its worldwide reserves are insufficient for large-scale industry.

Cobalt and iron are the metals which were proposed by Fischer and Tropsch as the first catalysts for syngas conversion. Both cobalt and iron catalysts have been used in the industry for hydrocarbon synthesis. A brief comparison of cobalt and iron catalysts is given in Table 1. Cobalt catalysts are more expensive, but they are more resistant to deactivation. Although the activity at low conversion of two metals is comparable, the productivity at higher conversion is more significant with cobalt catalysts. Water generated by FT synthesis slows the reaction rate on iron to a greater extent than on cobalt catalysts. At relatively low temperatures (473-523 K), chain growth probabilities of about 0.94 have been reported [Jager , 1998,Espinoza, 1999] for cobalt-based catalysts and about 0.95 for iron catalysts. The water-gas shift reaction is more significant on iron than on cobalt catalysts. The water-gas shift reaction is an important industrial reaction. It is often used in conjunction with steam reforming of methane or other hydrocarbons [Andrei Y. Khodakov, 2007].

The water-gas shift reaction:

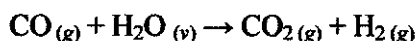


Table 1: Comparison of Cobalt and Iron FT Catalysts

Parameter	Cobalt Catalysts	Iron Catalyst
Cost	More expensive	Less expensive
Lifetime	Resistant to deactivation	Less resistant to deactivation (coking, carbon deposit, iron carbide)
Activity at low conversion	Comparable	
Productivity at high conversion	Higher; less significant effect of water on the rate of CO conversion	Lower, strong negative effect of water on the rate of CO conversion
Maximal chain growth propability	0.94	0.95
Water gas shift reaction $\text{CO} + \text{H}_2\text{O} \rightarrow + \text{H}_2$	Not very significant; more noticeable at high conversion	Significant
Maximal sulfur content	<0.1 ppm	<0.2 ppm
flexibility (temperature and pressure)	Less flexible; significant influence of temperature and pressure on hydrocarbon selectivity	Flexible; methane selectivity is relatively low even at 613 K
H ₂ /CO ratio	~2	0.5-2.5
Attrition resistance	Good	Not very resistant

Iron catalysts usually produce more olefins. Both iron and cobalt catalysts are very sensitive to sulfur, which could readily contaminate them. For iron-based catalysts, the syngas should not contain more than 0.2 ppm of sulfur. For Co catalysts, the amount

of sulfur in the feed should be much less than 0.1 ppm. [Dry, M. E, 2002] Cobalt catalysts supported on oxide supports are generally more resistant to attrition than iron coprecipitated counterparts; they are more suitable for use in slurry-type reactors. Iron catalysts produce hydrocarbons and oxygenated compounds under different pressures, H₂/CO ratios, and temperatures (up to 613 K). Cobalt catalysts operate at a very narrow range of temperatures and pressures; an increase in temperature leads to a spectacular increase in methane selectivity. Iron catalysts seem to be more appropriate for conversion of biomass-derived syngas to hydrocarbons than cobalt systems because they can operate at lower H₂/CO ratios [Andrei Y. Khodakov, 2007].

Both Co and Fe are used in combination with a range of supports and promoters that permit further control over the products selectivity. There are a few types of supports that can be used for the FTS. Silica is commonly used as a support material for Co because of its high surface area [D. Song, 2006] and also is often used as an (oxide) support for comparison with carbon. Recently, carbon was cited as a good candidate for FT synthesis, because lower Co-support interactions relative to silica lead to lower reduction temperature and better Co dispersion [Bezemer G.L, 2006]. A cited disadvantage of supporting cobalt on silica is that the strong Co precursor-silica interaction leads to a high reduction temperature, at which significant Co sintering occurs [Bezemer G.L, 2006]. The use of carbon as support for cobalt has been motivated by its potentially weaker interaction with the cobalt complexes, which would allow a lower reduction temperature and minimize sintering [Bezemer G.L, 2006]. Using CNT, based on paper by Bezemer et al. 2006, reported that particle size of cobalt FTS catalysis seems to have a threshold value of 6 nm and for silica supported cobalt catalysts, average cobalt particle size of 4.6±0.8 nm. So this study chooses the carbon nanotube (CNT) as the support.

A feasible methodology that has been developed for controlling the property of a metal is alloying. In particular, it has been experimented that the combination of active Fe and Co in the catalyst have generated product streams in the FT reaction richer in olefins and alcohols than the outcome of either single Fe or Co catalyst.

2.3 Strong electrostatic adsorption (SEA)

The method of strong electrostatic adsorption (SEA) as a simple, rational approach to synthesizing highly dispersed metals on oxide and carbon supports [J.R. Regalbuto, 2006]. The SEA method is based on an electrostatic mechanism in which the functional groups (typically hydroxyl) on the support surface can be protonated and deprotonated and thus positively or negatively charged as a function of pH. That pH at which the surface is neutral is designated the point of zero charge (PZC). The PZC is an important characterization parameter in order to optimize loading and anchor the metal complex precursor to maximize dispersion (high dispersion and anchoring of the precursor leads to *high dispersion of the metal on reduction*). At extreme low or high pH, adsorption is inhibited over all surfaces by high ionic strength [W.A. Spieker, 2001].

It has been suggested that molecular control of electrostatic adsorption might be achieved by changing the support PZC by doping with cations to increase the PZC, e.g., Na⁺ on silica, or by doping with anions to decrease the PZC, e.g., Cl⁻ on alumina. This works, in so far as PZC change is concerned, but does not affect the electrostatic adsorption of metal complexes (because there is dissolution and reversal of the doping effect) [J. Korah, 2003]. The oxidation of a carbon support, on the other hand, is reasonably irreversible in the absence of strong reducing agents and can be tuned by both the oxygen loading and the mix of functionalities formed by nitric acid oxidation and modified by reduction. Liquid phase oxidation mainly produces carboxylic acids while gas phase oxidation mainly produces hydroxyl and carbonyl groups [J.L. Figueiredo, 1999].

The PZC value of CNT is 3.7 [Sungchul Lee, 2011]. Support contains hydroxyl groups on its surface. In a pH < PZC medium, the hydroxyl groups will protonate and become positively charged and thus attracting anions. When pH > PZC, the hydroxyl groups will deprotonate and become negatively charged and attracting cations show in figure 2. At the pH of strongest interaction, oppositely charged metal coordination complexes adsorb in well-dispersed monolayers; in many cases, the high dispersion of

the precursor phase can be retained as the precursor is reduced to metal [J.R. Regalbuto, 2006]. In other words, pH value plays an important role in the deposition of metal precursor. Moreover this method can attract more metallic particles and increase the distribution to the base surface.

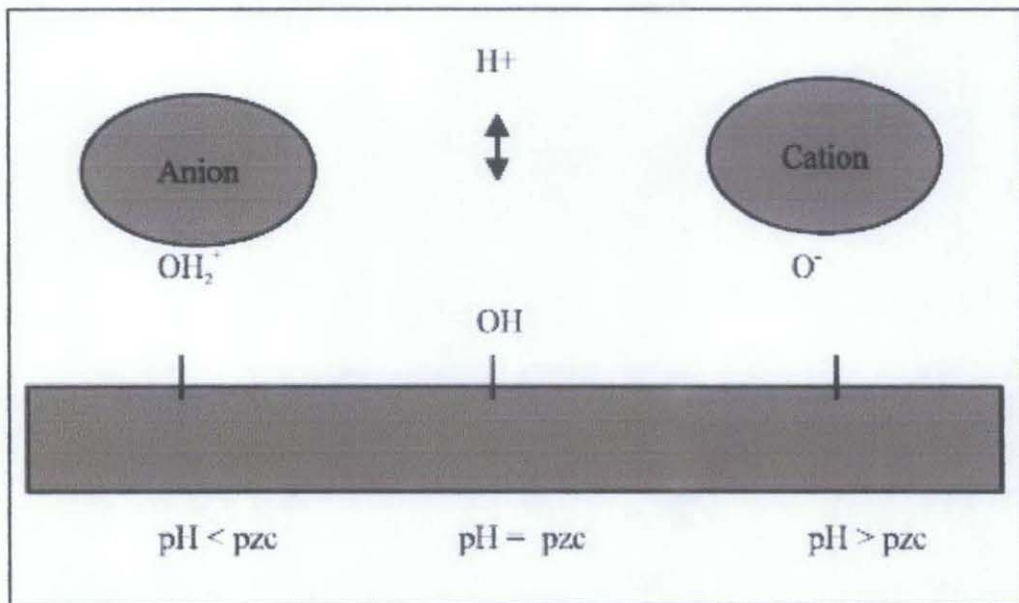


Figure 2: Mechanism of strong electrostatic adsorption (SEA) method

CHAPTER 3 METHODOLOGY

3.1 Methodology

Below is the methodology and flow chart of experiment:

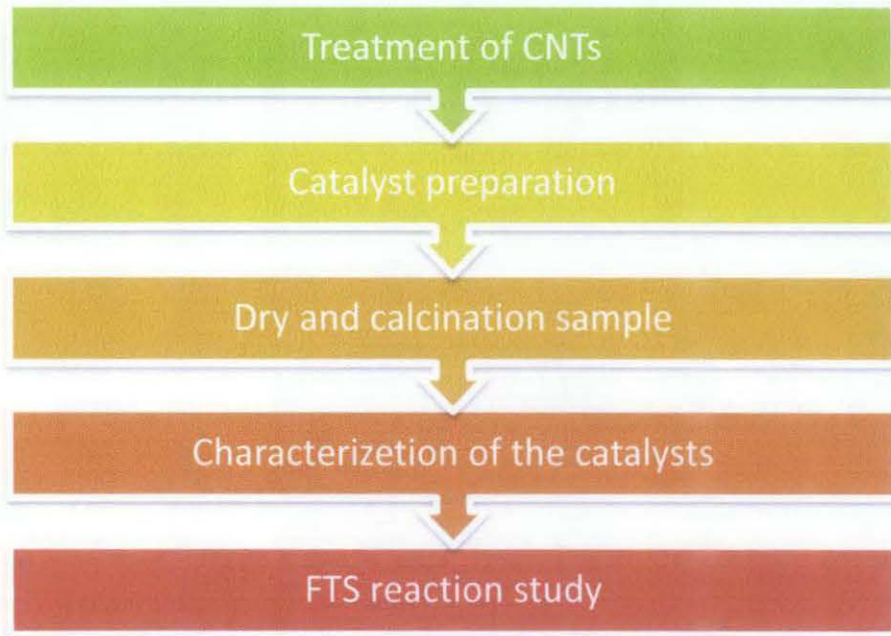


Figure 3: Flow chart of experiment procedure

3.2 Experimental

3.2.1 Treatment of CNTs

1. Prepare a 100ml HNO_3 (35%) solution.

$$M_1v_1 = M_2v_2$$

$$65\%v_2 = 35\% \times 100\text{ml}$$

$$v_1 = \frac{35\% \times 100\text{ml}}{65\%}$$

$$v_1 = 53.8 \text{ ml}$$

2. Set up the reflux apparatus as shown in figure 4.

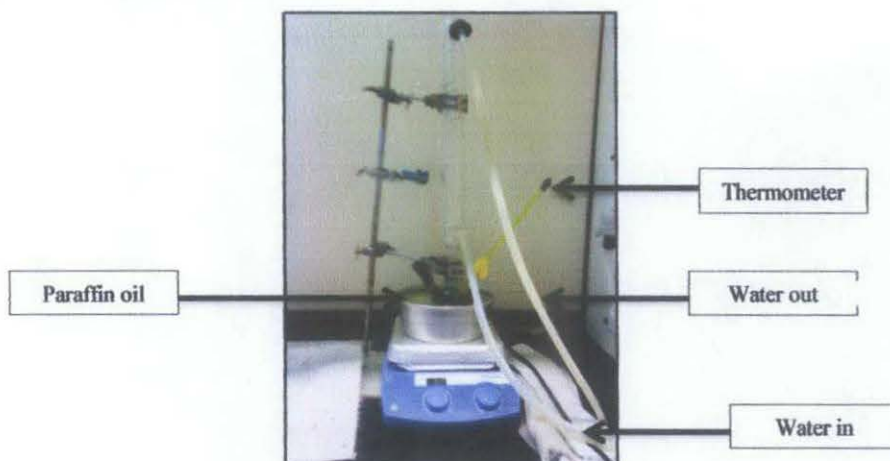


Figure 4: CNTs pretreatment process

3. Treat 3 grams Mknano-MWCNT (>95%) with 35 wt. % HNO_3 at 100°C for 16 hours.
4. After that, turn off the heater.
5. Let the water still circulate through the condenser until the temperature cooled down to ambient temperature.
6. Wait for the CNTs to settle down and filter off the HNO_3 .
7. Filter and wash CNTs with deionized water until the pH is neutral using the vacuum pump. (caution: careful with HNO_3 and CNTs)

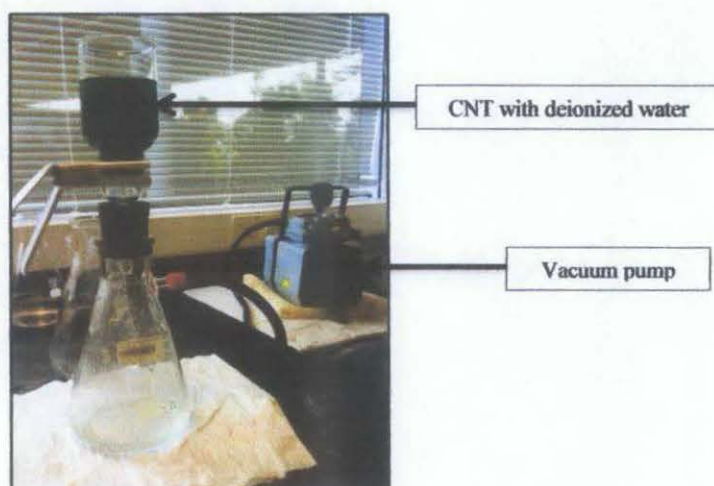


Figure 5: Washing process

8. Dry it at 120°C for 6 hours.

3.2.2 Catalyst preparation

1. Cobalt nitrate salt (Merck, 99.9% purity) and iron nitrate salt (Merck, 99.9% purity) are used as precursor to prepare the catalysts. (The PZC value of CNT is 3.7 [Sungchul Lee, 2011])
2. Cobalt and iron precursors are adsorb on the CNT support from an excess solution (to prevent pH shift) at various ratio of cobalt and iron metal like in the table below:

Table 2: Composition of Fe VS Co (5 wt. %)

Sample	S1	S2	S3	S4
Composition	100:0	90:10	80:20	70:30
Cobalt nitrate (g)	0.123	0.111	0.09	0.085
Iron nitrate (g)	0	0.02	0.04	0.054
CNTs(g)	0.475	0.475	0.475	0.475
Total (g)	0.593	0.606	0.605	0.614

3. Adjust pH of 50ml of deionized water to 8-9 using ammonia.
4. Add 0.475g CNT.
5. Add CoNO_3 and then FeNO_3 into the solution and stirred for 1 hour.



Figure 6: Stirred the solution for an hour

6. Label the sample with S1, S2, S3 and S4.

7. Filter the sample using filter paper.
8. Put it in the oven and dry the sample at 120°C for 6 hours.
9. Followed by calcination at 370°C in nitrogen flow using furnace Carbolite for 5 hours.



Figure 7: Calcination process using furnace Carbolite

3.2.3 Catalysts characterization

1. Use Transmission Electron Microscope (TEM) to analyze the morphology and size of the sample. The CNTs and catalysts were characterized by Transmission Electron Microscopy (TEM). Sample specimens for TEM studies were prepared by ultrasonic dispersion of the CNTs and catalysts in ethanol. The suspensions were dropped onto a carbon-coated copper grid
2. Field Emission Scanning Electron Microscope (FESEM-EDX)
3. Surface area analyzer (BET). This analytical technique uses physical adsorption and capillary condensation principles to determine surface area and porosity of solid materials.
4. Temperature-programmed reduction (TPR) is a widely used tool for the characterization of metal oxides, mixed metal oxides, and metal oxides dispersed on a support.
5. Use micro-tubular fixed-bed reactor at atmospheric pressure to study activity and selectivity of sample. ($H_2/CO = 2:1$ molar ratio, $P = \text{Atmospheric}$ and $T = 220\text{ }^\circ\text{C}$)

3.3 Tools Required

3.3.1 Chemicals

- i. Mknano-MWCNT (>95%)
- ii. 30 wt.% HNO₃
- iii. Ammonia
- iv. (Co(NO₃)₂).6H₂O 99 wt.% (Merck)
- v. (Fe(NO₃)₃).9H₂O 99 wt.% (Merck)

3.3.2 Equipment

- i. Vacuum pump
- ii. Furnace Carbolite
- iii. Transmission Electron Microscope (TEM)
- iv. Field Emission Scanning Electron Microscope (FESEM-EDX)
- v. Surface area analyzer (BET).
- vi. Temperature-programmed reduction (TPR)
- vii. Micro-tubular fixed-bed reactor

3.4 Project's Gantt chart and key milestone

No	Detail / Week	1	2	3	4	5	6	7		8	9	10	11	12	13	14	
1	Project Work Continues	Process	Mid-Semester Break														
2	Progress Report Submission									Key milestone							
3	Project Work Continues									Process	Process	Process					
4	Pre- EDX											Key milestone					
5	Draft Report Submission												Key milestone				
6	Dissertation Submission (soft copy)													Key milestone			
7	Submission of Technical Paper														Key milestone		
8	Oral Presentation															Key milestone	
9	Project Dissertation Submission (hardbound)																Key milestone



Process



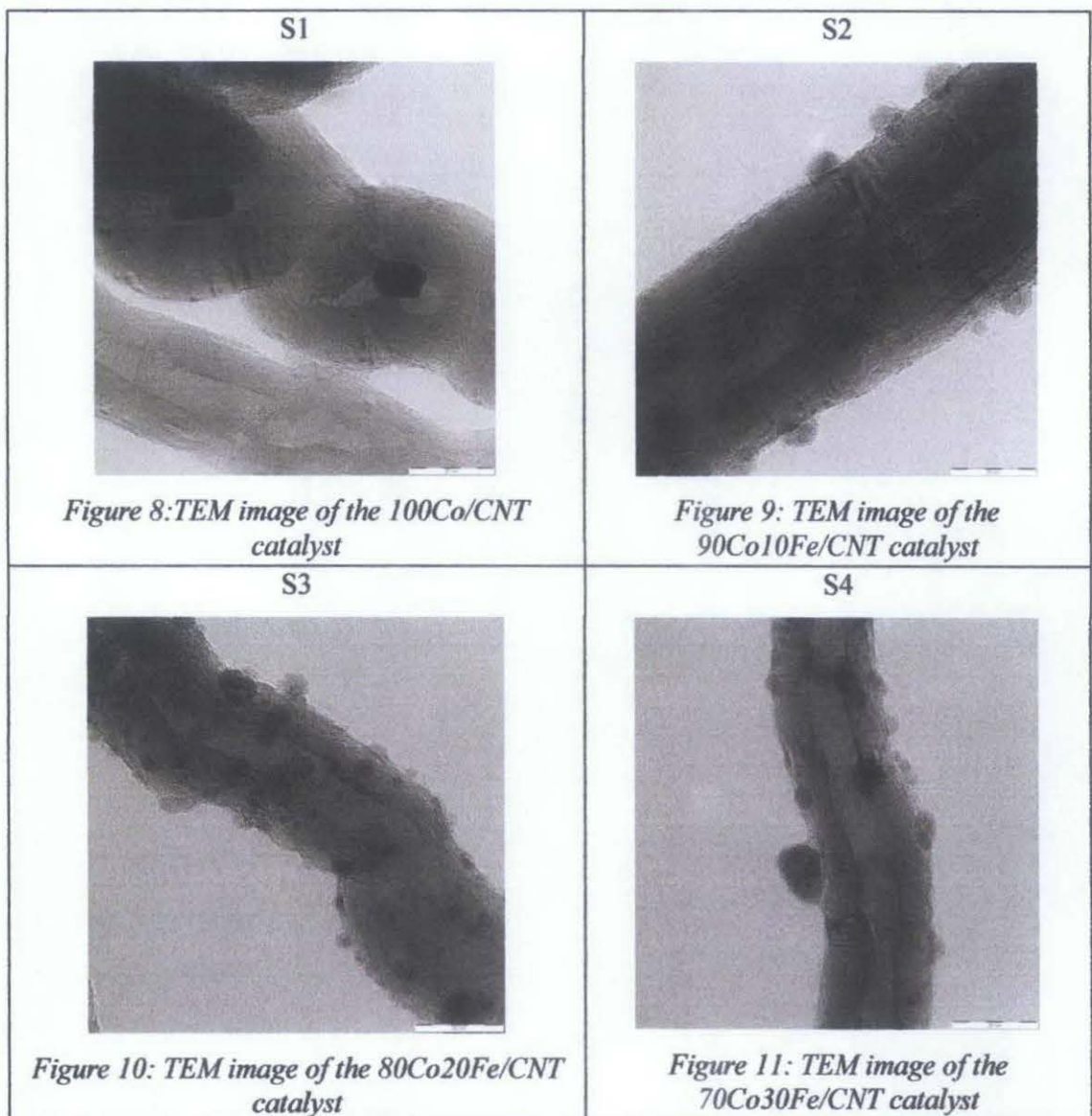
Key milestone

CHAPTER 4

RESULT AND DISCUSSION

4.1 Transmission Electron Microscope (TEM)

The sample of catalyst on CNTs was analyzed by TEM. Sample S1 is a 100Co/CNT catalyst. The TEM image revealed that the catalyst particles were dispersed inside the CNT. Sample S2 is a 90Co10Fe/CNT catalyst. The TEM image shows that the catalyst particles were dispersed inside the tubes and also on the external surface of the tube walls. Similar distributions of nanoparticles were observed for sample S3 and S4.



Based on the TEM image, particles that distribute inside and outside the CNT for each sample can be calculate as shows in the table

Table 3: Numbers of particles for each sample

Sample	No. of particle inside the CNT	Percentage (%)	No. of particle outside the CNT	Percentage (%)
S1	2	100	-	0
S2	4	30.8	9	69.2
S3	4	12.1	29	87.9
S4	3	21.4	11	78.6

From table 3, 100% of particles dispersed inside the CNT for sample S1, 30.8% inside and 69.2% outside the CNT for sample S2, 12.1% inside and 87.9% outside the CNT for sample S3, 21.4% inside and 78.6% outside the CNT for sample S4.

The bar graph depicting the size distribution of the total particles inside and outside the CNT was determined based on total particle population taken from several TEM micrographs. The fig. 12, 100% of the nanoparticles were in range 13-15nm inside the CNT for 100Co/CNT catalyst (S1). The average size of the particles inside the CNT is 13.5nm and standard deviation is 1.5nm.

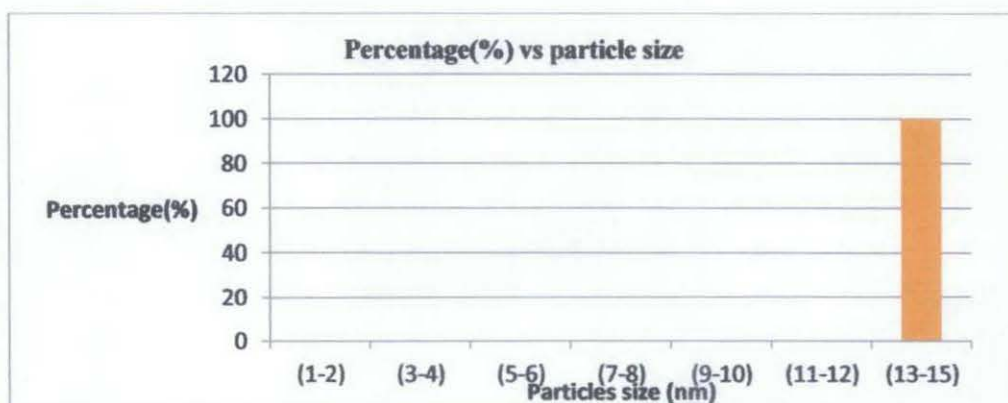


Figure 12: Particles size distribution for 100Co/CNT catalyst (inside CNT)

Fig. 13 and 14 shows particle size distribution for 90Co10Fe/CNT catalyst (S2). Fig. 13 shows that 75% of catalyst particles are in range 5-6nm and 25% in range 7-8nm been distributed inside the tube. The average size of the particles inside the CNT is 5.75nm and standard deviation is 0.74nm.

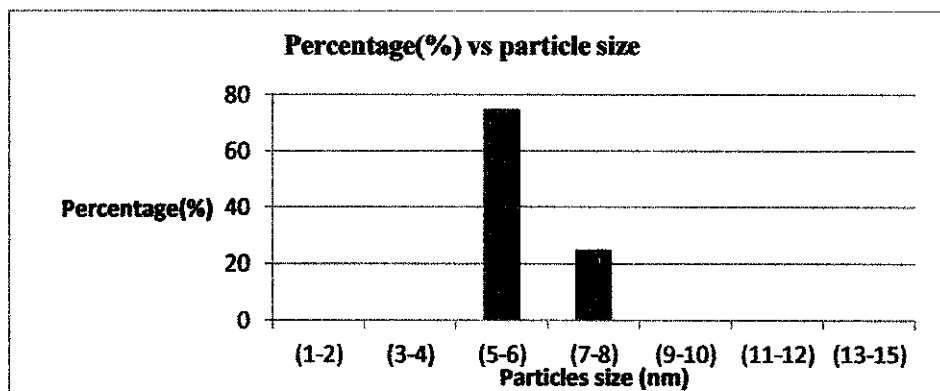


Figure 13: Particles size distribution for 90Co10Fe/CNT catalyst (inside CNT)

Fig 14 shows the distribution of catalyst particles outside the tube that are 22% in range 3-4nm, 22% in range 5-6nm, 11% in range 7-8nm and 45% in range 9-10. Average size of the particles deposited outside of CNT is 6.94nm and standard deviation is 2.43nm.

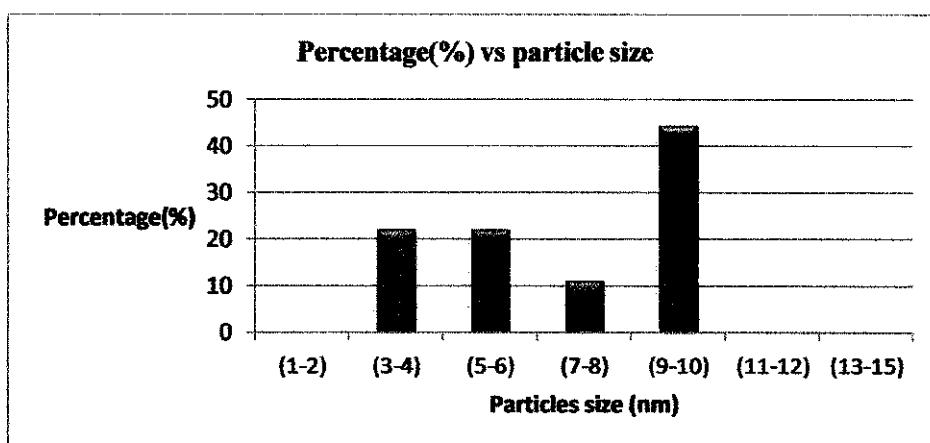


Figure 14: Particles size distribution for 90Co10Fe/CNT catalyst (outside CNT)

Fig. 15 and 16 shows particle size distribution for 80Co20Fe/CNT catalyst (S3). Fig 15 show the distribution of catalyst particles inside the tube that are 50% in range 5-

6nm and 50% in range 7-8nm. The average size of the particles inside the CNT is 6.25nm and standard deviation is 0.83nm.

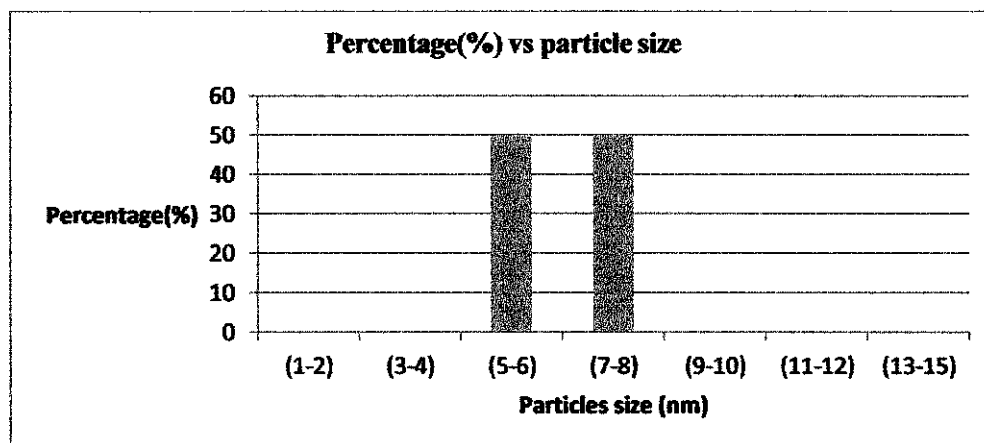


Figure 15: Particles size distribution for 80Co20Fe/CNT catalyst (inside CNT)

Fig 16 shows the distribution of catalyst particles outside the tube that are 3% in range of 1-2nm, 28% in range 3-4nm, 45% in range 5-6nm, 14% in range 7-8nm and 7% in range 9-10nm and 3% in range 13-15nm. Average size of the particles deposited outside of CNT is 5.67nm and standard deviation is 2.3nm.

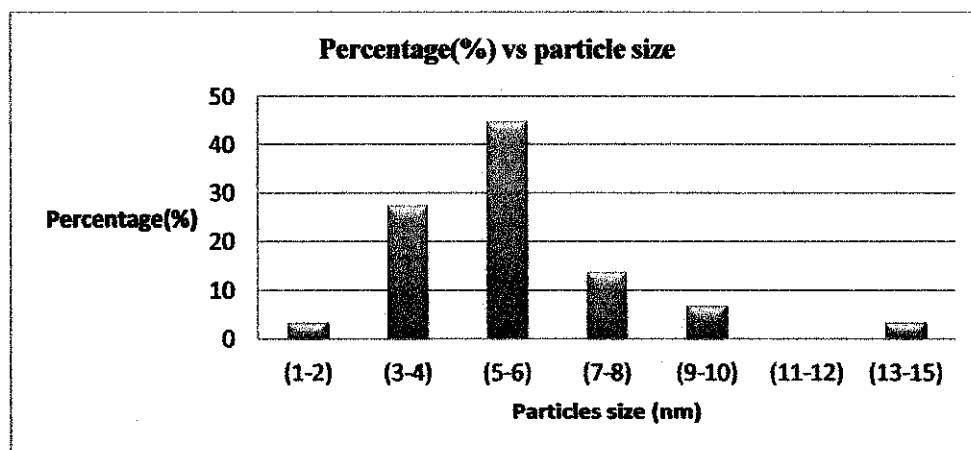


Figure 16: Particles size distribution for 80Co20Fe/CNT catalyst (outside CNT)

Figure 17 and 18 shows particles size distribution for 70Co30Fe/CNT catalyst (S4). Fig 17 show the distribution of catalyst particles inside the CNT that are 33.3% in range 5-6nm and 66.7% in range 7-8nm. The average size of the particles inside the CNT is 6.67nm and standard deviation is 0.47nm.

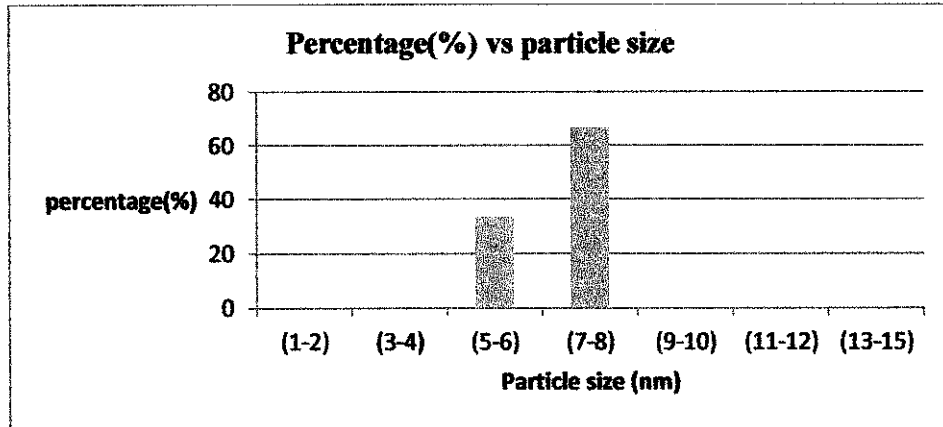


Figure 17: Particles size distribution for 70Co30Fe/CNT catalyst (inside CNT)

Fig 18 show the distribution of catalyst particles outside the CNT that are 7% in range 1-2nm, 21.5% in range 3-4nm, 18.2% in range 7-8nm and 21.5% in range 9-10nm and 7% in range 13-15nm. Average size of the particles deposited outside of CNT is 7nm and standard deviation is 3.38nm.

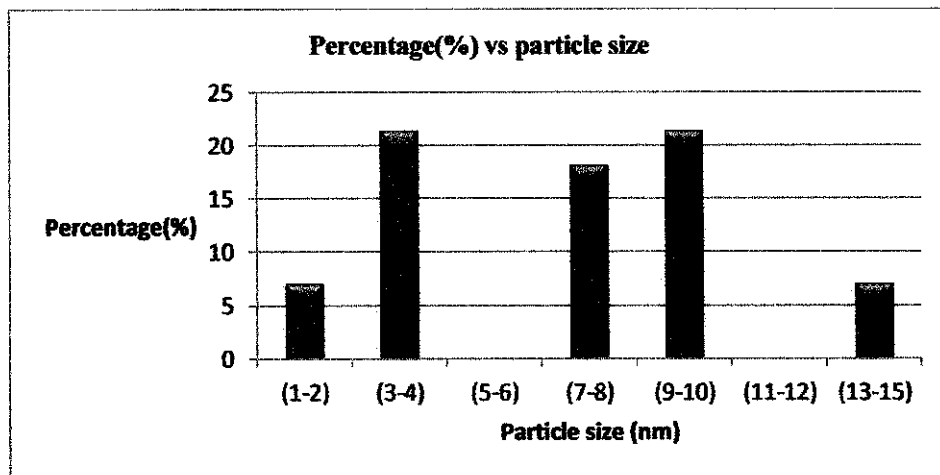
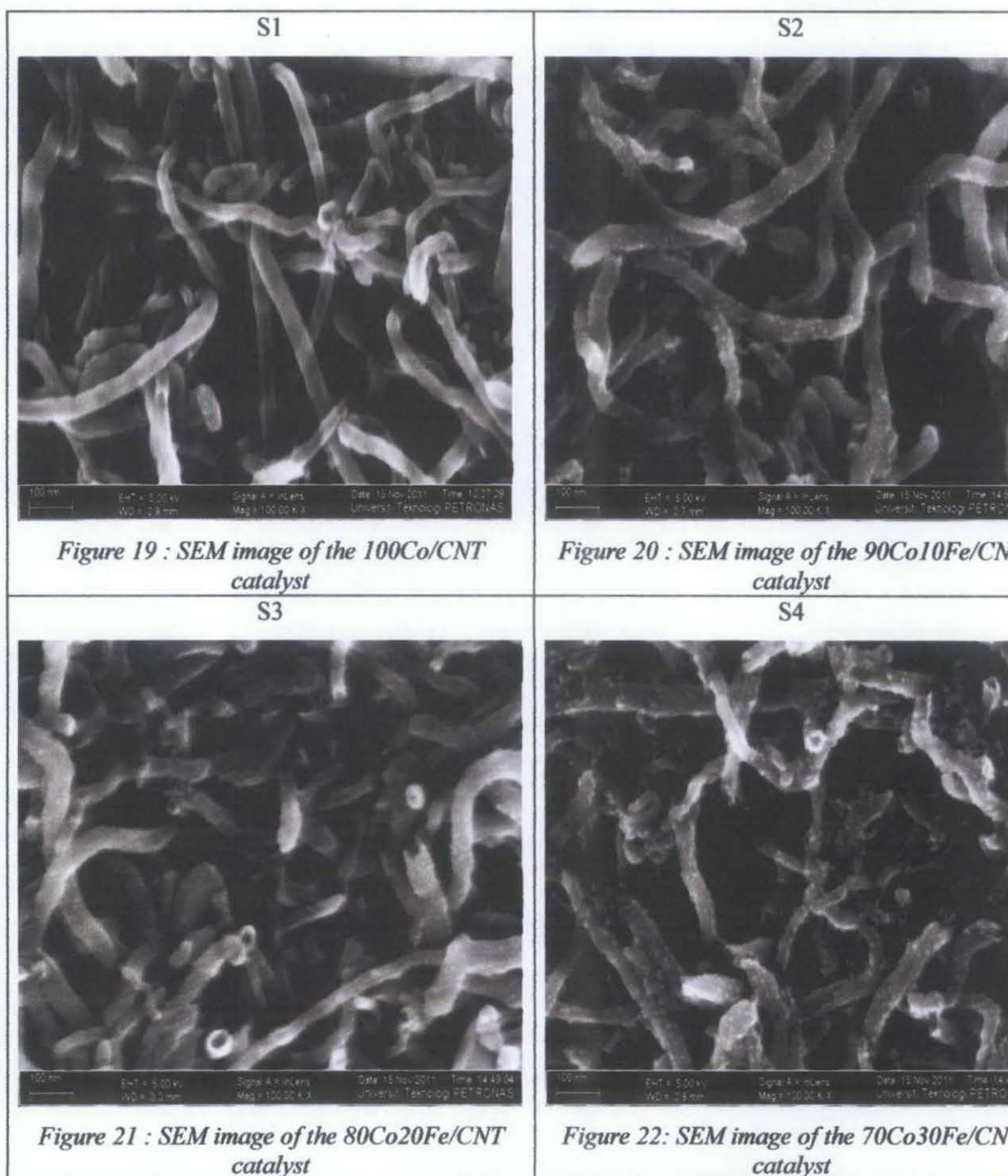


Figure 18: Particles size distribution for 70Co30Fe/CNT catalyst (outside CNT)

4.2 Field Emission Scanning Electron Microscope (FESEM-EDX)

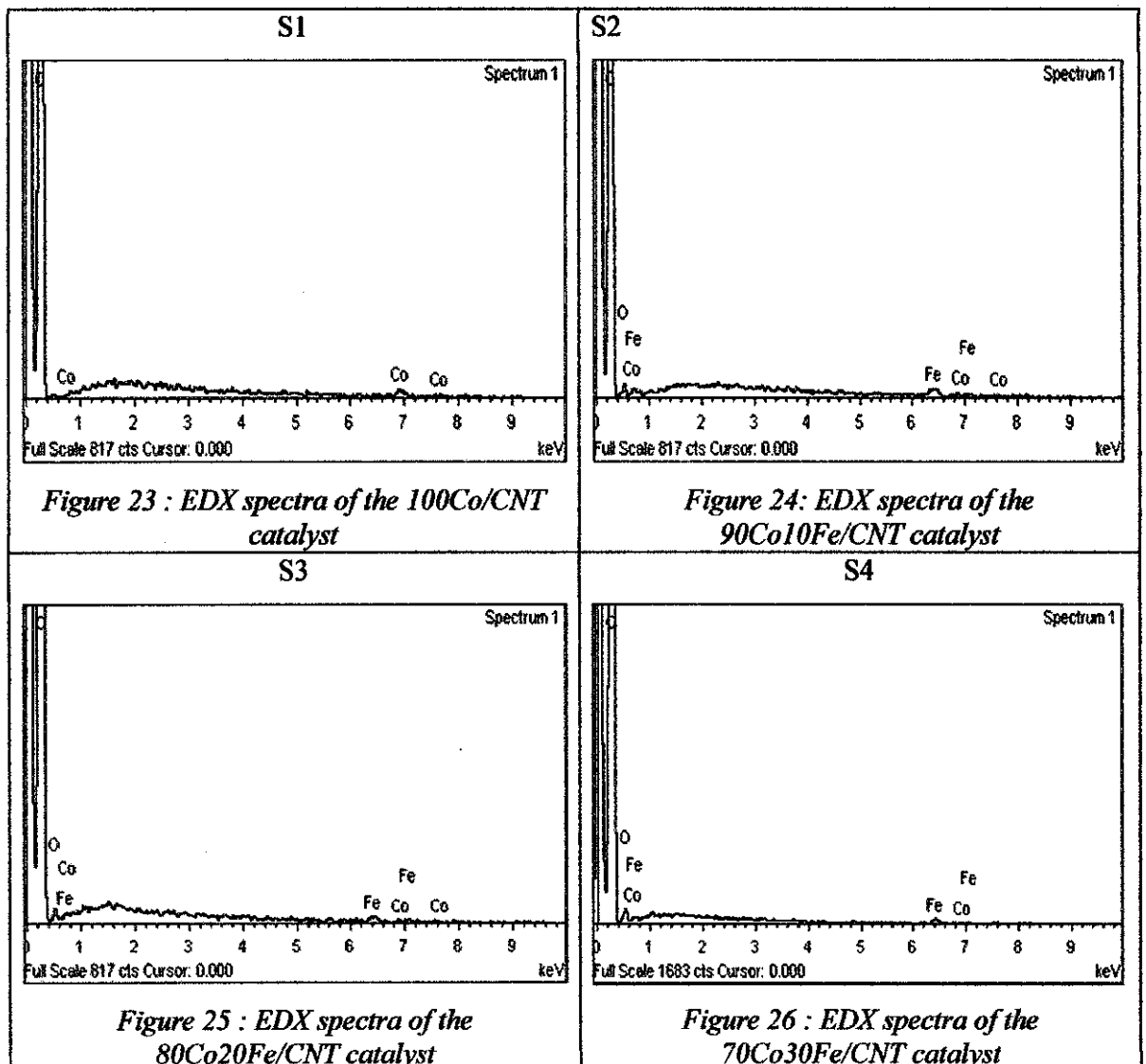
The SEM image of the entire sample shown below:



It was discovered 100 wt. % cobalt that has no particles distributed on the CNTs surface. For the 10 wt. % of iron loading, resulted in relatively small and uniformly

distributed particles on the CNTs surface. At 20 wt. % of iron loading, more of the CNTs surfaces were covered with particles and at 30 wt. % of iron loading, there were bigger particles dispersed on the CNTs surface.

The composition was studied using energy-dispersive X-ray (EDX).As shown in figure 23 for sample 1, the cobalt particles are present at 0.8 keV, 6.9 keV and 7.7 keV.



The results for sample 2, 3 and 4 have the same pattern. The cobalt particles are present at 7.6 keV for sample and iron particles are present at 6.5 keV. The peak at 6.9 keV can also be attributed to a new phase containing both cobalt and iron metals,

according to Kozhuharova et al. This phase may show that iron and cobalt interact strongly and formed Co-Fe alloy.

Table 4 shows the percentage of element for all samples. With addition of 10wt% of iron, the cobalt is 0.11% and iron is 1.79%. The percentage of cobalt and iron particles decreased with the increasing of iron loading. At 30 wt. %, the cobalt is 0.08% and iron is 0.58%.

Table 4: percentage of element for each composition

Composition	Wt.% of element			
	Co	Fe	O	C
S1	1.06	-	-	98.94
S2	0.11	1.79	7.16	90.94
S3	0.05	0.25	3.40	96.30
S4	0.08	0.58	5.47	93.87

4.3 Surface area analyzer (BET)

Results of surface area measurement are shown in table 5. The surface area for sample 1 was found to be 99m²/g and with incorporation of 10% of Fe, surface area decreased by 5%. While an opposite trend was observed for other catalysts formations in case of 80:20, 70:30 surface area increased by 9% and 4% respectively.

The pore volume decreased from 0.39 to 0.33 with increasing the percentage of iron metal. Incorporation of cobalt and iron to CNTs support led to an increasing in BET areas and decreasing pore volume, and pore blockage with increasing amount of Fe.

Table 5 : BET surface area and porosity data for catalysts.

Support/catalyst	BET (m ² /g)	Pore volume (single point) (cm ³ /g)	Average pore diameter(nm)
100% Co 0%Fe CNT	99	0.36	14.3
90% Co 10% Fe CNT	94	0.39	16.7
80%Co 20%Fe CNT	108	0.36	13.4
70%Co 30Fe CNT	103	0.33	12.7

4.4 Temperature programmed reduction (TPR)

The activation of the catalyst in hydrogen atmosphere was disclosed by temperature programmed reduction (TPR) experiments. The TPR profile of the calcined catalysts and CNTs support are shown in figure 27.

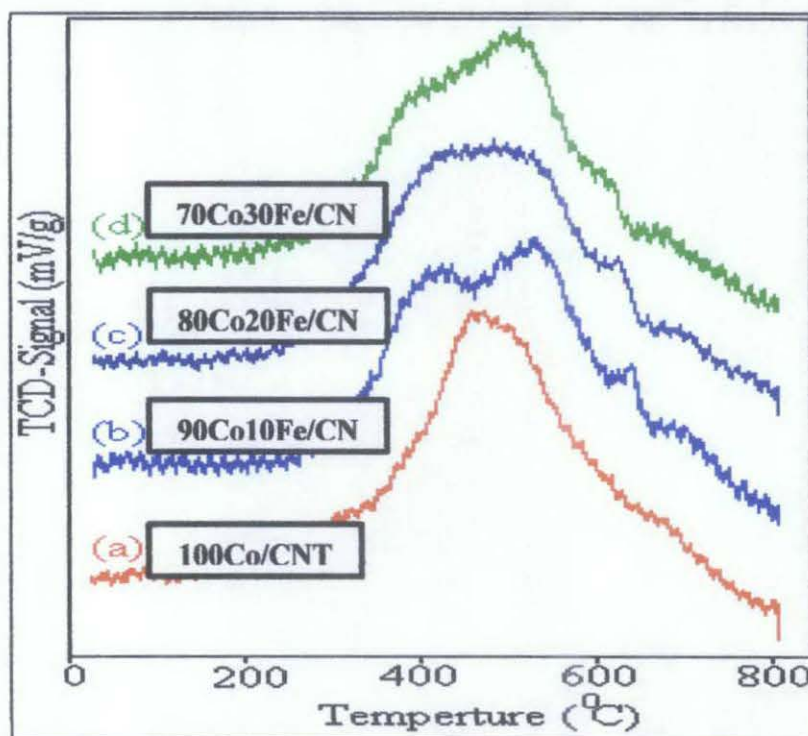


Figure 27: TPR profiles of 100Co/CNT, 90Co10Fe/CNT, 80Co20Fe/CNT and 70Co30Fe/CNT

The first peak of the TPR profile of the catalyst was assigned to the reduction of Co_3O_4 to CoO , and the second peak with a broad shoulder was mainly assigned to the second reduction step, which is the reduction of CoO to Co^0 [A.Tavasoli, 2008]. This peak also included the reduction of catalyst species that interact with the support, which extend the TPR profile to higher temperatures [A.Tavasoli, 2008]. The graph of 100Co/CNT shows a single peak at 490°C. This means that Co_3O_4 is reduced to Co^0 just in a single reduction step. There is a single reduction peak at 450°C. The second graph is 90Co10Fe/CNT shows two peaks. The first reduction peak is at 420°C and the second reduction peak is at 540°C. A similar pattern of graph is observed for 80Co20Fe/CNT and 70Co30Fe/CNT. The figure 27 also shows that the first reduction peak of

80Co20Fe/CNT and are at 70Co30Fe/CNT 420°C and 395°C and second reduction peak are at 500°C and 520°C.

The small peak at about 650°C at the TPR profile of 90Co10Fe/CNT catalyst, 645°C at TPR profile of 80Co20Fe/CNT and 640°C at TPR profile of 70Co30Fe/CNT were assigned to the gasification of the support. It has been suggested that this new peak at the reduction profile of these catalysts with a broad tailing could be related to the formation of a very stable, difficult-to-reduce Fe rich phase, which may be formed in the synthesis of the bimetallic catalysts [D.J. Duvenhage, 1997].

4.5 Micro-tubular fixed-bed reactor

The catalysts had been test using microtubular fixed-bed reactor for catalytic activity and product selectivity. The catalysts were evaluated in terms of their Fischer–Tropsch synthesis (FTS) activity (g HC produced/g cat./h) and selectivity (the percentage of the converted CO that appears as a hydrocarbon product) in a fixed bed micro-reactor. Prior to the activity tests, the catalyst activation was conducted according to the following procedure. The catalyst (0.02 g) was placed in the reactor and pure hydrogen was introduced at a flow rate of 10 ml/min. The reactor temperature was increased from room temperature to 370 °C at a rate of 10 °C/min, maintained at this activation condition for 14 h and the catalyst was reduced in-situ. After the activation period, the reactor temperature was decreased to 180 °C under flowing hydrogen.

Synthesis gas with a flow rate of 10 ml/min (H₂/CO ratio of 2) was introduced at the top of the fixed bed reactor and the reactor pressure was increased to 2 MPa. The reactor temperature was then increased to 220 °C at a rate of 10 °C/min. Products were continuously removed from the reactor and passed through two traps, one maintained at 100 °C (hot trap) and the other at 0 °C (cold trap). The uncondensed vapor stream was reduced to atmospheric pressure through a pressure letdown valve.

The % CO conversion is shown in the figure 29. The 100Co/CNT is the highest CO conversion which is 11.5%. %CO conversion decreases to 2.5% with addition of iron to cobalt catalyst with Fe loading of 10 wt. %. An opposite trend was observed for other catalysts formations in case of 80:20, 70:30 increased to 6.6% and 7.03% respectively.

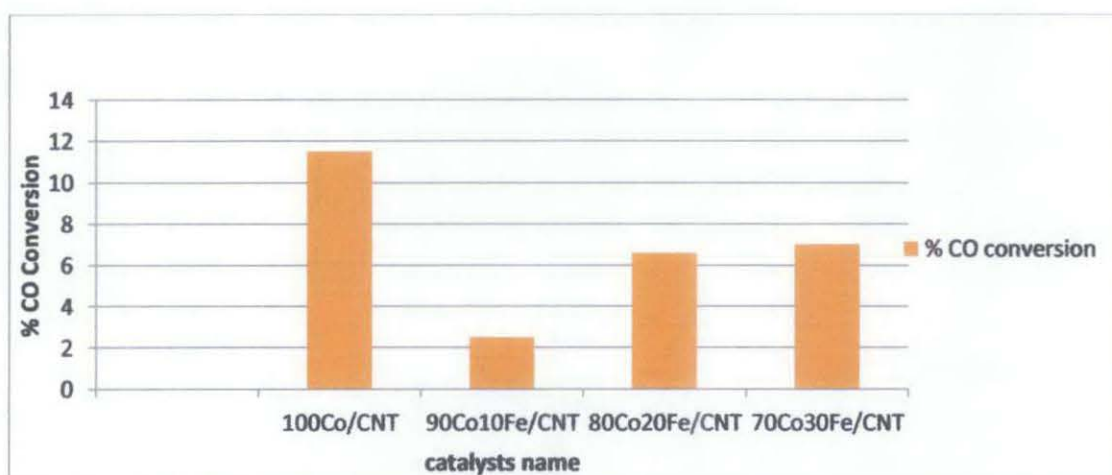


Figure 29: %CO conversion for catalysts

Product selectivity of the catalysts is displayed in the figure 30. Comparing the hydrocarbon selectivity over the 90Co10Fe/CNT and 80Co20Fe/CNT with the 100Co/CNT catalyst, both S2 and S3 shows high selectivity to C₂-C₄ and for 90Co10Fe/CNT catalyst it is produce C₅⁺ hydrocarbon.

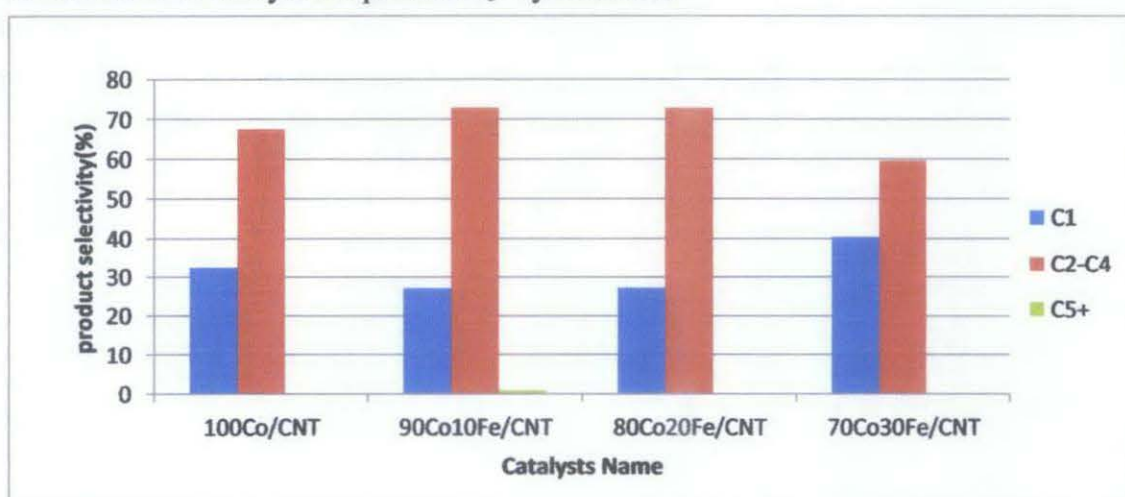


Figure 30 : Product selectivity of catalysts

CHAPTER 5

CONCLUSION AND RECOMMENDATION

5.1 Conclusion

Bimetallic nanocatalysts supports on CNTs of Co-Fe were successfully synthesized using the strong electrostatic adsorption (SEA) method but it was not a good catalyst for FTS in term of product selectivity. It was found that incorporation of Fe modified the physicochemical properties of Co-catalysts. The effects of Co/Fe ratio on the activity and selectivity of Co-Fe bimetallic catalysts were studied. A series of catalyst containing Fe and Co on carbon nanotubes was prepared, and FT studies revealed that the two metals, when intimately mixed together, had different catalytic characteristics than catalysts containing only one of the Co metals. The image obtained by TEM and SEM showed most of the metal particles were homogeneously distributed on the outer surface of the CNTs. The product selectivity increased remarkably with addition of small amount of iron to cobalt catalyst where a highest hydrocarbon was obtained for the 90Co10Fe/CNT is C_5^+ that is 0.85%.

5.2 Recommendation

Strong electrostatic adsorption (SEA) method has potential to optimize the nanocatalyst performance for FTS. Further studies should be conducted using different temperature and pressure for the activity and product selectivity test. During the catalysts preparation, shake the solution for a longer time to improve the distributions of particles inside the CNT and also can try at the different pH.

REFERENCES

- Andrei Y. Khodakov, Wei Chu, and Pascal Fongarland “Advances in the Development of Novel Cobalt Fischer-Tropsch Catalysts for Synthesis of Long-Chain Hydrocarbons and Clean Fuels”. *Chemical Review*, 2007, volume 107, pp 1692–1744.
- A.Tavasoli, K.Sadagiani, F.Khorashe and al, “Cobalt supported on carbon nanotubes—a promising novel Fischer–Tropsch synthesis catalyst”. *Fuel Processing Technology* 89 (2008) 491–498.
- Bezemer G.L., J.H. Bitter, H.P.C.E. Kuipers, H. Oosterbeek and J.E. Holewijn, 2006. “Cobalt particle size effects in the fischer-tropsch reaction studied with carbon nanofiber supported catalysts”. *J. Am. Chem. Soc.*, 128: 3956-3964.
- Bezemer G.L., P.B. Radstake, V. Koot, A.J. van Dillen, J.W. Geus, K.P. de Jong, J. “On the origin of the cobalt particle size effect in the fischer-tropsch synthesis” *Catal.* 237 (2006) 291.
- Chee Kai Ling, Noor Asmawati Mohd. Zabidi and Chandra Mohan, 2011. “Synthesis and Characterization of Silica-Supported Cobalt Nanocatalysts Using Strong Electrostatic Adsorption”. *Journal of Applied Sciences*, 11: 1436-1440.
- Den Breejen, J.P., P.B. Radstake, G.L. Bezemer, J.H. Bitter, V. Froseth, A. Holmen and K.P. de Jong, 2009. “On the origin of the cobalt particle size effects in
- D.J. Duvenhage, N.J. Coville, “Fe: 10/TiO₂ bimetallic catalysts for the Fischer–Tropsch reaction I.” *Characterization and reactor studies, Appl. Catal., A Gen.* 153 (1997) 43–67.
- Dry, M. E. “The Fischer-Tropsch process: 1950-2000” *Catal. Today* 2002, 71, 227.
- D. Song, J. Li, J. Mol. “Effect of catalyst pore size on the catalytic performance of silica supported cobalt Fischer–Tropsch catalysts”. *Catal. A Chem.* 247 (2006) 206–212.
- Espinoza, R. L.; Steynberg, A. P.; Jager, B.; Vosloo, A. C. “Low temperature Fischer-Tropsch synthesis from a Sasol perspective”. *Appl. Catal. A* 1999, 186 (1-2), 13.

Jager, B. "Developments in Fischer-Tropsch technology". *Stud. Surf. Sci. Catal.* 1998, 119, 25.

Jager, B.; Espinoza, R. "Advances in low temperature Fischer-Tropsch synthesis". *Catal. Today* 1995, 23, 17.

Jiao, L. and J.R. Regalbuto, 2008.: "The synthesis of highly dispersed noble and base metals on silica via strong electrostatic adsorption" I. *Amorphous silica*. *J. Catal.*, 260: 329-341.

J. Korah, W.A. Spieker, J.R. Regalbuto,. "Why Ion-Doped, PZC-Altered Silica and Alumina Fail to Influence Platinum Adsorption" *Catal. Lett.* 85 (2003) 123–127.

J.L. Figueiredo, M.F.R. Pereira, M.M.A. Freitas, J.J.M. Órfão, "Modification of the surface chemistry of activated carbons". *Carbon* 37 (1999) 1379–1389.

J.R. Regalbuto, "A scientific method to prepare supported catalysts, in: R. Richards (Ed.), *Surface and Nanomolecular Catalysis*", *Taylor & Francis, London*, 2006, chap. 6.

J.R. Regalbuto, "Preparation of supported metal catalysts by strong electrostatic adsorption (SEA)", in: *Handbook of Catalyst Preparation*, *Taylor & Francis, London*, 2006, chap. 18.

J.T. Miller, M. Schreier, A.J. Kropf, J.R. Regalbuto, "Studies in Surface Science and Catalysis" *J. Catal.* 225 (2004).

Regalbuto, J.R., 2007. "Catalyst Preparation: Science and Engineering". *CRC Press, Boca Rotan, FL.*, pp: 474.

R. Kozhuharova, M. Ritschel, D. Elefant, A. Graff, I. Monch, T. Muhl, C.M. Schneider, A. Leonhardt, "(FexCo1-x)-alloy filled vertically aligned carbon nanotubes grown by thermal chemical vapor deposition", *J. Magn. Magn. Mater.* 290–291 (2005)

S.Sun, N.Tsubaki and K. Fujimoto: “Different Functions of the Noble Metals Added to Cobalt Catalysts for Fischer–Tropsch Synthesis” *J. Chem. Eng. Jpn. Vol.* 33(2000)p.232

Sungchul Lee, Zhiteng Zhang, Xiaoming Wang, Lisa D. Pfefferle, Gary L. Haller.
“Characterization of multi-walled carbon nanotubes catalyst supports by point of Zero charge”. *Catalysis Today*, 164 (2011) 68–73

Vannice, M. A. 1975 “The catalytic synthesis of hydrocarbons from H_2/CO mixtures over the Group VIII metals : V. The catalytic behavior of silica-supported metals” *J. Catal.*, 37, 449.

W.A. Spieker, J.R. Regalbuto, “A fundamental model of platinum impregnation onto alumina” *Chem. Eng. Sci.* 56 (2001) 3491–3504.